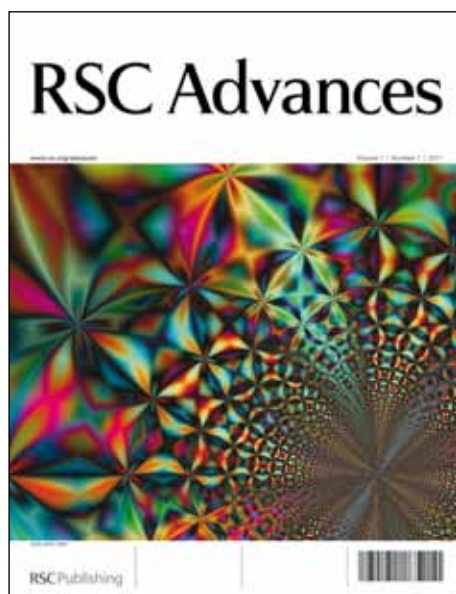


# RSC Advances

## Accepted Manuscript

This article can be cited before page numbers have been issued, to do this please use: K. H. Rahme, M. T. Nolan, T. Doody, G. McGlacken, M. A. Morris, C. O'Driscoll and J. Holmes, *RSC Adv.*, 2013, DOI: 10.1039/C3RA41873A.



This is an *Accepted Manuscript*, which has been through the RSC Publishing peer review process and has been accepted for publication.

*Accepted Manuscripts* are published online shortly after acceptance, which is prior to technical editing, formatting and proof reading. This free service from RSC Publishing allows authors to make their results available to the community, in citable form, before publication of the edited article. This *Accepted Manuscript* will be replaced by the edited and formatted *Advance Article* as soon as this is available.

To cite this manuscript please use its permanent Digital Object Identifier (DOI®), which is identical for all formats of publication.

More information about *Accepted Manuscripts* can be found in the [Information for Authors](#).

Please note that technical editing may introduce minor changes to the text and/or graphics contained in the manuscript submitted by the author(s) which may alter content, and that the standard [Terms & Conditions](#) and the [ethical guidelines](#) that apply to the journal are still applicable. In no event shall the RSC be held responsible for any errors or omissions in these *Accepted Manuscript* manuscripts or any consequences arising from the use of any information contained in them.

# Highly Stable PEGylated Gold Nanoparticles in Water: Applications in Biology and Catalysis

Kamil Rahme,<sup>\* a,b,c</sup> Marie Therese Nolan,<sup>d</sup> Timothy Doody,<sup>e</sup> Gerard P. McGlacken,<sup>d</sup> Michael A. Morris,<sup>a,b</sup> Caitriona O'Driscoll<sup>e</sup> and Justin D. Holmes<sup>a,b</sup>

<sup>a</sup>Materials Chemistry and Analysis Group, Department of Chemistry and the Tyndall National Institute, University College Cork, Cork, Ireland.

<sup>b</sup>Centre for Research on Adaptive Nanostructures and Nanodevices (CRANN), Trinity College Dublin, Dublin 2, Ireland.

<sup>c</sup>Department of Sciences, Faculty of Natural and Applied Science, Notre Dame University (Louaize), Zouk Mosbeh, Lebanon

<sup>d</sup>Organic and Pharmaceutical Chemistry Group, Department of Chemistry and Analytical and Biological Chemistry Research Facility, UCC, Cork, Ireland

<sup>e</sup>Pharmacodelivery group, School of Pharmacie, University College Cork, Cork, Ireland.

\*To whom correspondence should be addressed: Fax:+961 9 225164; Tel:+961 9 218950

E-mail: [kamil.rahme@ndu.edu.lb](mailto:kamil.rahme@ndu.edu.lb)

†Electronic Supplementary Information (ESI) available: [details of any supplementary information available should be included here].

**ABSTRACT:**

Here we report the synthesis of well dispersed gold nanoparticles (Au NPs), with diameters ranging between 5-60 nm, in water and demonstrate their potential usefulness in catalysis and biological applications. Functionalised polyethylene glycol-based thiol polymers (mPEG-SH) were used to stabilise the pre-synthesised NPs. Successful PEGylation of the NPs was confirmed by Dynamic Light Scattering (DLS) and Zeta potential measurements. PEG coating of the NPs was found to be key to their colloidal stability in high ionic strength media compared to *bare* citrate-stabilised NPs. Our results show that PEG-Au NPs with diameters < 30 nm were useful as catalysts in the homocoupling of arylboronic acids in water. Additionally, PEG-Au NPs were also shown to be stable in biological fluids, and not cytotoxic on B16.F10 and CT-26 cell lines, and able to successfully deliver siRNA to CT-26 cells, achieving a significant reduction ( $p < 0.05$ ) in the expression levels of luciferase protein; making these NPs attractive for further biological studies.

**KEYWORDS:** Gold nanoparticles, homocoupling, stabilisation, polyethylene glycol (PEG), cytotoxicity, cell association and siRNA delivery.

## Introduction

The increasing progress of nanotechnology in the last few decades has made nanomaterials indispensable in many areas such as material science, medicals, and cosmetics.<sup>1-3</sup> Nanoparticles (diameter 1-100 nm) exhibit particular properties that arise from quantum size effects and also from a high surface to volume ratio.<sup>1, 4, 5</sup> Their small size enable them to interact with biomolecules (such as enzymes, antibodies, DNA, proteins etc.) and cells.<sup>6</sup> As such, they are of appropriate dimensions for applications in nanobiotechnology and catalysis.<sup>7-9</sup> Noble metal nanoparticles, especially gold, are well known for their characteristic surface plasmon resonances which form the basis for many biological sensing and imaging applications.<sup>1, 4, 10-13</sup> Besides their potential applications in biology, the catalytic application of gold nanoparticles (Au NPs) in organic reactions has also been of considerable interest in recent years. Important transformations using Au catalysis, such as the selective oxidation of alcohols,<sup>14-16</sup> CO oxidation in the absence of H<sub>2</sub>,<sup>17-19</sup> chemoselective reduction of nitroarenes,<sup>20</sup> and a wide variety of commercially important synthetic protocols have been studied extensively.<sup>21-23</sup> Researchers have also shown that poly(2-aminothiophenol) (PATP)-supported Au NPs can be used in Suzuki-Miyaura cross-coupling reactions.<sup>24</sup> More recently, the homocoupling of arylhalides has been accomplished using a catalytic system comprising of Au NPs supported on a bifunctional periodic mesoporous organosilica.<sup>25</sup> Aryl boronic acids have also been homocoupled using Au on solid supports through apparent heterogeneous conditions. Homocoupling with high selectivity was achieved using Au supported on CeO<sub>2</sub>.<sup>26</sup> The applications of nanoparticles in biology and catalysis typically requires them to be well dispersed and stable in solution, which can be difficult due to their high surface energies.<sup>27</sup> Due to this instability especially in presence of salts NPs can lose their size-dependent properties (catalytic, optical, magnetic *etc.*) caused by the high tendency of adhesion and aggregation.<sup>28</sup> Aggregation of nanoparticles is much more pronounced in solvents with high ionic strengths, *i.e.* biological fluids, and in presence of other chemicals such as high concentration of salts that is one of the main causes of aggregation.<sup>12</sup> Therefore, the dispersion of NPs must be controlled to provide a better platform for the advancement of these materials in catalytic and biological applications.<sup>29</sup> In this

manuscript we report the synthesis of stable colloidal Au NPs in water and under physiological conditions (0.15 M NaCl), achieved by attaching polyethylene glycol-based thiol polymers (mPEG-SH) as a stabilising ligand to the surfaces of Au NPs, via thiol linkages. PEG was the ligand of choice due to its ability to inhibit non-specific interactions with proteins in biological applications, as well as its compatibility with a diverse set of solvents (water, DMSO, THF etc).<sup>30, 31</sup> Further applications of Au NPs-PEG were demonstrated in the homocoupling of boronic acids in water. Our data shows that the PEG-Au NPs, with diameters < 30 nm, were useful as catalysts in the homocoupling of arylboronic acids in water, while PEG-Au NPs, with diameters of 60 nm, and Au NPs-citrate nanoparticles of different sizes (5, 15, 30 and 60 nm) had minimal catalytic efficiency. Moreover, the catalytic efficiency of 15 nm Au NPs-PEG<sub>10000</sub>, expressed in term of the yield of pure 4-methoxyphenylboronic acid, was found to increase from 6 to 60 % when the amount of Au NPs increased from 0.48 to 5 mol %. Finally, the PEG-Au NPs were complexed with siRNA and also tested for toxicity on B16.F10 and CT-26 cell lines, either alone or in presence of siRNA, and for aptitude in delivering siRNA to CT-26 cell lines.

## Experimental

### Chemicals and materials.

Purified H<sub>2</sub>O (resistivity  $\approx$  18.2 M $\Omega$  cm) was used as a solvent. All glassware was cleaned with aqua regia (3 parts of concentrated HCl and 1 part of concentrated HNO<sub>3</sub>), rinsed with distilled water, ethanol, and acetone and oven-dried before use. Tetrachloroauric acid trihydrate (HAuCl<sub>4</sub>.3H<sub>2</sub>O), sodium citrate (C<sub>6</sub>H<sub>5</sub>Na<sub>3</sub>O<sub>7</sub>.2H<sub>2</sub>O), sodium borohydride (NaBH<sub>4</sub>) and ascorbic acid were purchased from Sigma Aldrich. Thiol terminated poly(ethylene glycol) methyl ether, M<sub>w</sub> = 2100, 5400; 10800 and 20800 g mol<sup>-1</sup>) were purchased from Polymer Source<sup>®</sup>. All products were used as received.

## Preparation and PEGylation of Gold Nanoparticles.

**Diameter of  $5 \pm 1.5$  nm Au NPs:** To an aqueous solution (150 mL) of  $\text{HAuCl}_4 \cdot 3\text{H}_2\text{O}$  ( $0.25 \text{ mmol L}^{-1}$ ) was added  $2.5 \mu\text{mol}$  of a  $200 \mu\text{M}$  mPEG-SH ( $M_w=10800 \text{ g mol}^{-1}$ ) solution and the mixture was stirred vigorously. To this solution were added an ice cold solution of  $\text{NaBH}_4$  in order to have a final concentration of  $0.25 \text{ mmol L}^{-1}$   $\text{NaBH}_4$ . After addition of  $\text{NaBH}_4$ , an instantaneous colour change from pale yellow to deep red was noted. The AuNPs obtained with this procedure were approximately  $5 \pm 1.5$  nm.

**Diameter of  $\sim 15 \pm 1.5$  nm Au NPs:** 150 mL of an aqueous solution of  $\text{HAuCl}_4 \cdot 3\text{H}_2\text{O}$  ( $0.25 \text{ mmol L}^{-1}$ ) was heated to  $95 \text{ }^\circ\text{C}$  with stirring.  $0.53 \text{ mL}$  of a  $340 \text{ mmol L}^{-1}$  sodium citrate aqueous solution was rapidly added. The colour of the solution changed from pale yellow to dark blue, and then to deep red-burgundy within about 8 min. Stirring and heating was maintained during 1.5 h after addition of sodium citrate. The heat was then removed and the solution was kept under stirring, until cooled to room temperature. The Au NPs obtained with this procedure were  $\sim 15 \pm 1.5$  nm.

Preparation of  $\sim 30 \pm 4$  nm and  $\sim 60 \text{ nm} \pm 8$  nm AuNPs: For Au NPs, larger than 15 nm, a weak reducing agent ascorbic acid was used. For  $\sim 30$  nm AuNPs, 150 mL of an aqueous solution of  $\text{HAuCl}_4 \cdot 3 \text{H}_2\text{O}$  ( $0.25 \text{ mmol L}^{-1}$ ) and  $1 \text{ mmol L}^{-1}$  sodium citrate was stirred vigorously. To this solution was added a volume of ascorbic acid in order to have a final concentration of  $0.38 \text{ mmol L}^{-1}$ . After addition of ascorbic acid the colour of the solution changed from pale yellow to dark blue, and then to deep red-burgundy in less than 1 min. Stirring and was maintained during 1h. The AuNPs obtained were  $30 \pm 4$  nm. By increasing the concentration of ascorbic acid to  $1 \text{ mmol L}^{-1}$ , added in 2 times sequence (0.5 each), AuNPs  $\sim 60 \text{ nm} \pm 8$  nm were obtained, we note that these AuNPs were less monodisperse.

**Grafting of Poly(ethylene glycol) Ligands.** Thiolated polyethylene glycol (mPEG-SH) was covalently grafted to the surface of the Au nanoparticles. A solution of mPEG-SH of the desired molecular weight

was added to a solution of citrate-capped Au nanoparticles with stirring. The solution was stirred for ~1 h allowing citrate ligands to exchange with mPEG-SH. The excess mPEG-SH was removed via centrifugation at 15 000 rpm for about 45 min. Thiol groups are known to have a strong affinity for Au, resulting in covalent attachment of PEG to the Au nanoparticles. The resulting colloidal solutions were very stable for several months, as well as in high ionic strength solvents and biological fluids, furthermore they were able to undergo filtration and freeze drying.

### **UV-visible Spectroscopy**

Optical absorption spectra were obtained on a CARY UV–visible spectrophotometer with a Xenon lamp (300–900 nm range, 0.5 nm resolution).

### **Dynamic light scattering and zeta potential measurements**

The pristine solutions of Au and PEGylated Au nanoparticles, were diluted by 5 to 10 times depending on the initial concentration (absorption range 0.2- 0.5) prior to dynamic light scattering (DLS) measurements. The measurements were undertaken with the Malvern instrument (Zeta sizer Nano Series) at 25 °C using the default non-invasive back scattering (NIBS) technique with a detection angle of 173°. Three measurements were made per sample and the standard deviation ( $\sigma$ ) was calculated, typically  $\sigma = 1-2$  nm.

### **Transmission electron microscopy**

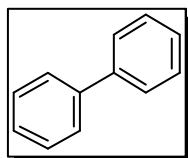
Citrate and PEG-stabilised Au nanoparticles were placed on carbon-coated copper grids (Quantifoil, Germany) and dried over night in air, prior to transmission electron microscope (TEM) inspection. The samples were inspected using a JEOL JEM-2100 TEM operating at 200 kV. All the micrographs were recorded on a Gatan 1.35 K × 1.04 K × 12 bit ES500W CCD camera. TEM images were analysed using Image J software.

## Scanning electron microscopy

Citrate and PEG-stabilised gold nanoparticles were deposited from solution on a silicon wafer and dried in air prior to inspection by scanning electron microscope (SEM). The samples were inspected using a FEI 630 NanoSEM equipped with an Oxford INCA energy dispersive X-ray (EDX) detector, operating at 5 kV.

## General protocol for homocoupling: Characterisation data:

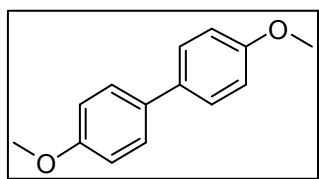
Synthesis of Biphenyl:



In a round bottom flask (100 mL) equipped with a condenser and magnetic stirrer bar, phenylboronic acid (2 mmol) and NaOH (8 mmol) were mixed with 15 nm Au NP-PEG<sub>2000</sub> (2 mol%) in H<sub>2</sub>O (40 mL). The resulting mixture was stirred at 80 °C for 48 h.

The crude reaction mixture was then extracted with ethyl acetate (3 × 20 mL). The organic layers were combined and washed with 10 % aqueous NaOH solution, dried with MgSO<sub>4</sub>, filtered and concentrated under reduced pressure to afford the pure product (67 mg, 44%) as a white solid, m.p. 67-68°C (lit.<sup>2</sup> 67-69°C);  $\lambda_{\max}/\text{cm}^{-1}$  (KBr): 3034, 1943, 1569, 1480, 1429, 729, 696;  $\delta_{\text{H}}$  (300 MHz) 7.61-7.57 [4H, m], 7.46-7.41 [4H, m], 7.39-7.31 [2H, m];  $\delta_{\text{C}}$  (CDCl<sub>3</sub>, 75.5 MHz) 141.26, 128.8, 127.3, 127.2.

Synthesis of 4,4'-dimethoxybiphenyl:



In a round bottom flask (100 mL) equipped with a condenser and magnetic stirrer bar, *para*-methoxy boronic acid (1 mmol) and NaOH (2 mmol) were mixed with 15 nm Au NP-PEG<sub>10 000</sub> (5 mol%) in H<sub>2</sub>O (25 mL). The

resulting mixture was stirred at 80°C for 22 h. The crude reaction mixture was then extracted with ethyl acetate (3 × 20 mL). The organic layers were combined and washed with 10 % aqueous NaOH solution, dried with MgSO<sub>4</sub>, filtered and concentrated under reduced pressure to afford the pure product (64.2 mg,

60%) as a white solid, m.p. 168-169°C (lit.<sup>3</sup> 168-170°C);  $\lambda_{\text{max}}/\text{cm}^{-1}$  (KBr)<sup>4</sup>:2958, 1500, 1439, 1276, 1249, 1041;  $\delta_{\text{H}}$  (300 MHz) 7.49-7.45 [4H, m], 6.98-6.93 [4H, m], 3.84 [6H, s];  $\delta_{\text{C}}$  (CDCl<sub>3</sub>, 75.5 MHz)158.7, 133.5, 127.7, 114.2, 55.4.

### NMR Spectroscopy (NMR)

NMR spectra were run in CDCl<sub>3</sub> using tetramethylsilane (TMS) as the internal standard. <sup>1</sup>H NMR spectra were recorded at 300 MHz on a Bruker AVANCE 300 spectrometer. <sup>13</sup>C NMR spectra were recorded at 75 MHz on a Bruker AVANCE 300 instrument.

### Infra-red spectroscopy (IR)

IR spectra were recorded on a Perkin-Elmer FT-IR Paragon 1000 spectrophotometer. Solid samples were dispersed in potassium bromide and recorded as pressed discs.

### Melting points

Melting points were measured in a Thomas Hoover Capillary Melting Point apparatus.

### Dynamic light scattering and zeta potential measurements in the presence of biomolecules

Au-PEG particles were complexed with siRNA or siRNA:Protamine at a molar ratio of 1:10. Samples were complexed for 1 h and subsequently diluted in either double distilled H<sub>2</sub>O or in Dulbecco's modified eagle's medium without phenol red (Sigma-Aldrich) prior to DLS and zeta potential analysis. Measurements were performed using a Zetasizer Nano from Malvern instruments at 25 °C (back

scattering at 173° NIBS default). The model used in the fitting procedure was provided by the instrument (using Mark Houwink parameters and cumulative fit). The standard deviation was calculated by performing three measurements on each sample.

### Cell culture, cytotoxicity and in vitro siRNA knockdown

*MTT Cytotoxicity Assay.* The murine melanoma stably expressing pGL4 luc2 lentivirus, B16-F10-luc2 (Caliper Life Sciences, Hopkinton, MA) were routinely cultured in RPMI 1640 supplemented with 10 % Foetal Bovine Serum and grown in 5 % CO<sub>2</sub> at 37 °C. Prior to cytotoxicity determination cells were seeded at a density of  $4 \times 10^4$  cells in a 96-well plate and grown in complete media for 24 h. Cell viability was determined by the MTT assay which measures the reduction of MTT to formazan by mitochondrial reductase enzymes giving a purple colour. Au NPs alone and protamine condensed siRNA (50nM) complexed with Au nanoparticles, were added to the cells and incubated for 4 h. The medium was removed and replaced with fresh complete medium containing MTT ((3-(4,5-dimethylthiazole-2-yl)-2,5-diphenyltetrazolium) bromide) (Sigma) at a working concentration of 0.5 mg/ml. After 4 h of incubation the cell culture medium was removed, and the formazan crystals produced were dissolved in 100 µl DMSO for 5 min at room temperature. Absorbance was read at a wavelength of 590 nm. A similar procedure described above was also performed on murine colon carcinoma cell line, CT26. All experiments were performed in triplicate.

### In vitro siRNA knockdown

*Cell Culture and in vitro siRNA knockdown.* The murine colon carcinoma cell line, CT26, was obtained from the American Type Culture Collection (ATCC). Cells were maintained in Dulbecco's modified Eagle medium (Sigma) supplemented with 10 % fetal bovine serum (Sigma). Cells were grown in 5 % CO<sub>2</sub> at 37 °C. For in vitro siRNA knockdown, cells were seeded, 24 h prior to transfection at a density

of  $5 \times 10^4$  cells in a 24 well plate. Cells were transfected with Luciferase reporter plasmid, pGL3Luc ( $1 \mu\text{g well}^{-1}$ ) complexed with Lipofectamine 2000 ( $3 \mu\text{l } \mu\text{g}^{-1}$  DNA) for 2 h. Cells were then washed twice with PBS prior to siRNA transfection. Luc GL3 siRNA (50 nM), was condensed with Protamine (MR5 – Mass Ratio), and subsequently complexed with Au NP's (MR10) or Lipofectamine 2000 ( $1 \mu\text{l } \mu\text{l}^{-1}$  siRNA). Luc GL3 siRNA alone and non-silencing siRNA were used as control. After 4 h, complexes were removed and fresh medium was added to each well. Cells were incubated for a further 20 h and luciferase was determined using a luciferase assay kit (Promega) according to the manufacturer's instructions. Luciferase expression levels were normalised to cell protein content as determined by BCA (bicinchoninic acid) protein assay (Pierce). Experiments were carried out in triplicate.

### Fluorescence microscopy

CT26 cells were seeded at a density of  $5 \times 10^4$  per well on glass cover slips in a 24 well plate and grown for 24 hr. Prior to addition of particles, cells were washed and fresh media was added. Fluorescently-labelled protamine condensed siRNA, complexed with Au NP's at MR 10, and control formulation (protamine condensed siRNA), were added to the cells and incubated for 20 h. The media was subsequently removed and the cells washed with cell scrub buffer (AMS Biotechnology). The cells were fixed for 15 min at room temperature in 3 % paraformaldehyde (PFA). The coverslips were washed twice with  $1 \times$  PBS at room temperature. Free aldehyde groups were quenched with 50 mM  $\text{NH}_4\text{Cl}$  solution at room temperature. Following two more washes with  $1 \times$  PBS, the coverslips were mounted on glass slides. Association of the particles with cells was assessed by fluorescent detection of the labeled siRNA using a Nikon Eclipse TS100 inverted microscope equipped with fluorescein and DAPI filters and Metamorph version 6.1 software.

## Results and Discussion

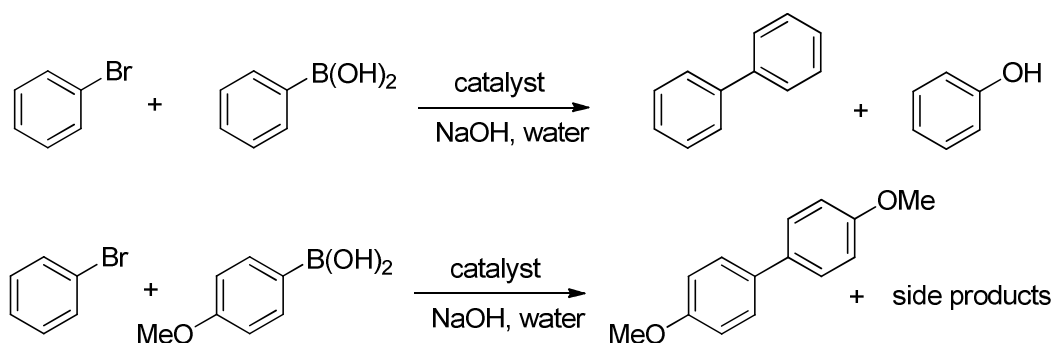
### Preparation and characterisation of PEG-AuNPs

Au NPs were synthesised with mean diameters of  $5 \pm 1.5$  nm,  $15 \pm 1.5$  nm,  $30 \pm 4$  nm and  $60 \pm 8$  nm in water by the controlled chemical reduction of a  $\text{HAuCl}_4$  solution. Different reducing agents were used to produce Au NPs in this study; the strong reducing agent sodium borohydride ( $\text{NaBH}_4$ ) was used at room temperature to produce Au NPs with a mean diameter of 5 nm; sodium citrate, a mild reducing agent, was used at high temperature to produce  $\sim 15$  nm Au NPs, and finally ascorbic acid, a weak reducing agent, was used at room temperature to produce Au NPs with mean diameters of 30 and 60 nm.<sup>34-37</sup> The physical properties of the Au NPs synthesised were characterised using uv-visible spectroscopy and either TEM or SEM (**Figure 1**). The uv-visible data clearly show that the NPs synthesised exhibited size dependent optical properties, resulting in a shift of the surface plasmon resonance (SPR) band from a wavelength of 514 to 534 nm, as the mean diameter of the Au NPs increased from 5 to 60 nm respectively.<sup>4</sup> TEM and SEM analysis of the NPs, utilising *Image J* software, showed a size polydispersity below 20 %, with the exception of the 60 nm Au NPs ( $\sim 30$  %). Electrostatically-stabilised NPs are very sensitive to changes in pH and ionic strength.<sup>12, 29, 38</sup> Therefore, to maintain an adequate dispersion of Au NPs in high ionic strength media, they were coated with the PEG-SH capping ligand directly after synthesis. The stability of the PEG-Au NPs under physiological conditions ( $0.157 \text{ mol.L}^{-1}$  NaCl), was monitored by uv-visible spectroscopy (**Figure 2**) and the number of PEG-SH ligands needed to coat the surface of a Au NP of a particular diameter was estimated.<sup>39</sup> The grafting density was also determined by TGA and TEM.<sup>39</sup> Our data have shown that Au NPs-PEG hybrids were very stable when compared to *bare* citrate-stabilised Au NPs in the presence of NaCl (see Supporting Information, Figure S1). Following the addition of salt to the citrate-stabilised Au NPs, the initial red colour of the colloidal solution immediately turned blue, due to a shift of the SPR peak at  $\sim 520$  nm to 532 nm, with the immediate appearance of a second band at  $\sim 690$  nm after 1 minute, attributed to a change in the dispersion of the Au NPs-citrate solution in presence of NaCl (0.157 M). A

further shift to higher wavelength, ~ 710 nm after 20 minutes, ~ 722 after about 1 hour and finally ~734 nm after 2 hours, was also observed. This continuous shift was accompanied by a decrease in the absorption of the overall UV-visible spectra over the time (Figure 2a), that can be attributed to citrate-stabilised Au NPs aggregation.<sup>12, 29, 40</sup> No nanoparticles were observed in solution after 3-4 hours and a black precipitate was detected visually after this time period (Figure 2a). However, the PEG-stabilised Au NPs were only slightly affected by the addition of salt to the dispersion and no colour change of the solution was observed (Figure S1), due to their high stability in high ionic strength conditions. Figure 2b shows the spectrum of Au NPs-PEG<sub>10 000</sub> before (t = 0), 1 minute, 3 and 24 hours after adding NaCl. The successful PEGylation of the Au NPs was also confirmed by DLS/Zeta potential measurements in presence of salt. **Figure 3(a)** shows DLS analysis for 15 nm Au NPs functionalised with various mPEG-SH ligands molecular weight at different polymer concentrations. The mean diameter of the Au NPs was observed to increase with the PEG concentration in all cases. This increase was more pronounced as the length of the PEG capping ligand increased, *i.e.* Au NPs-citrate size increased from 19.8 to 41 nm when coated with PEG<sub>10 000</sub>. However, the size increase was less pronounced with the shorter PEG<sub>2 000</sub>, indicating that more polymer was grafted onto the Au NPs before reaching surface saturation (plateau). A similar trend was seen for the Zeta potential measurements **Figure 3 (b)**. We note that TGA performed in a previous study, has also shown that the number of PEG ligands grafted on ~15 nm AuNPs increases when the PEG length decreases.<sup>39</sup> The hydrodynamic diameter increases with the PEG length inducing a thicker PEG layer which shields the surface charges, providing good stability.<sup>12, 29, 39, 40</sup> In addition, the PEG-Au NPs did not aggregate significantly in the presence of NaCl and other salts. DLS/Zeta combined with TEM analysis, provided full characterisation of the colloidal dispersion for further applications.

## PEG-AuNPs catalytic efficiency

We initially tested *bare* 5, 15, 30 and 60 nm Au NPs-citrate as catalysts under Suzuki-Miyaura-type conditions. When bromobenzene, phenyl boronic acid and NaOH were heated in water (95-100 °C) the colour of the solution changed from red to blue, indicating that the citrate-stabilised Au NPs aggregated under these conditions. In all experiments, less than 2 % conversion to biaryl products was always observed, similar results of about 2 % conversion were also obtained in the absence of Au NPs, indicating that Au NPs-citrate has no catalytic efficiency under the above conditions. Similarly, our potential catalyst Au NP size  $15 \pm 1.5$  nm, PEG-SH 10800 was tested under Suzuki-Miyaura-type conditions. Again, we observed that a significant amount of starting materials remained unreacted as judged from analysis of the NMR spectra of our crude reaction mixture. However pure biphenyl was isolated in trace amounts ( $\sim 2$  %, **Scheme 1**). To test if homocoupling rather than cross-coupling was occurring, we repeated the reaction using bromobenzene and *p*-MeO-phenylboronic acid. To our surprise no cross-coupled product was observed with only homocoupled product, arising from homocoupling of *p*-MeO-phenylboronic acid, isolated in 9 % yield.



**Scheme 1.** Gold-catalyzed heterocoupling reaction of bromobenzene with phenylboronic acid or 4-methoxyphenylboronic acid.

Based on these data, a number of optimisation experiments were undertaken, as shown in **Table 1**, for the homocoupling of *para*-methoxy phenylboronic acid. In order to test the effect of the concentration of the Au catalyst on the reaction yield, 15 nm Au NPs-PEG<sub>10,000</sub> were used for the homocoupling of *p*-methoxyphenyl boronic acid in the presence of sodium hydroxide. The Au catalyst loading was varied

(4.87, 6.25, 10, 25 and 50  $\mu\text{mol}$  or 0.48, 0.62, 1, 2.5 and 5 mol %) and the isolated yield of the pure 4,4'-dimethoxybiphenyl product was found to be 6, 9, 25, 49 and 60 % respectively (**Figure 4**). Finally, to check the effect of the PEG length, Au NPs-PEG<sub>10,000</sub> were compared to the Au NPs-PEG<sub>20,000</sub> in the homocoupling reaction of *p*-methoxyphenyl boronic acid and under similar conditions; our results did not show a big difference in the yield obtained of the pure products.

### **Stability in biological media and in presence of biomolecules, AuNPs/cells interaction, and cytotoxicity**

PEG-Au NPs were complexed with siRNA in order to test their toxicity in the presence and absence of siRNA. Due to the anionic nature of the Au NPs, negatively charged naked siRNA will not readily bind to the particles. To allow binding, GL3 Luciferase siRNA was first complexed with protamine (a positively charged peptide) at MR 5 producing complexes with an overall positive charge facilitating electrostatic interaction with the negatively charged nanoparticles. Zeta potential measurements showed an increase in charge from  $-1.9 \pm 1.4$  mV for siRNA alone, to  $42 \pm 1.15$  mV when complexed with protamine. Complexes were produced with a range of Au NPs at MR 10 (Au:(siRNA:Protamine)). These complexes exhibited a nearly neutral surface charge, and their sizes were slightly increased when compared to uncomplexed Au NPs (See Table S1).

The viability of CT26<sup>39</sup> and B16.F10 cells after treatment with the Au NPs was determined by the MTT assay. Cells were treated with a range of Au NPs complexed with protamine condensed siRNA at biologically active concentrations (**Figure 5**). None of the PEG-coated Au nanoparticles synthesised in this study exhibited any cytotoxicity in B16.F10 or CT26 cell cultures, either alone or complexed with siRNA.<sup>39</sup> Association with cells is vital for NP aided siRNA delivery. The protamine:siRNA complexation to the Au NPs does not have a significant effect on the toxicity of Au NPs. Protamine:siRNA on its own also does not exhibit any toxicity. The physical characteristics of the PEG-Au NPs were conserved after complexation with siRNA/protamine as no change in the colour of the

colloidal solutions was observed after bioconjugation. However, a slight increase in the diameter of the 15 nm Au nanoparticles was observed after complexation with siRNA/protamine, as confirmed by DLS (**Table S1**). The increase in the NP diameter was most likely due to weak interactions between neighbouring nanoparticles. However, this interaction was not strong enough to release the ligands from the surface of the NPs to allow direct core-core interaction.

### **Complexation with siRNA, characterization, and siRNA delivery.**

PEG-Au NPs were complexed with siRNA in order to test their usefulness as a delivery vector. Due to the anionic nature of the Au nanoparticles negatively charged, naked siRNA will not readily bind to the particles. To allow binding, GL3 Luciferase siRNA was first complexed with protamine (a positively charged peptide) at MR 5 producing complexes with an overall positive charge facilitating electrostatic interaction with the negatively charged nanoparticles. Zeta potential measurements showed an increase in charge from  $-1.9 \pm 1.4$  mV for siRNA alone, to  $42 \pm 1.15$  mV when complexed with protamine. Complexes were produced with a range of Au NPs at MR 10 (Au:(siRNA:Protamine)). These complexes exhibited a positive surface charge, and their sizes were slightly increased when compared to uncomplexed Au NPs. For example, the 15 nm PEG<sub>2,100</sub> particles increased in size from  $28 \pm 1.5$  nm (Table 1) to  $46.95 \pm 5.25$  nm upon complexation of siRNA. A similar increase in size was noted when complexes were measured in transfection media (15 nm PEG<sub>2,100</sub> size increased to  $138 \pm 4.19$ ). This increase was not, however, seen for larger Au NPs, *e.g.* the size of 30 nm PEG<sub>10,800</sub> was  $72.8 \pm 4$  nm before complexation,  $69.69 \pm 0.5$  nm after siRNA complexation and  $69.91 \pm 0.6$  nm when measured in transfection media. When assessing the loading of siRNA to cationic particles a gel retardation assay can be utilised.<sup>41,42</sup> This method cannot, however, be utilised in the case of protamine:siRNA binding to the gold particle as the complexation of the siRNA with protamine itself causes gel retardation and protects the siRNA from EtBr intercalation. Further studies to determine the extent of binding of the

protamine:siRNA complex will be carried out in the future and these studies will include modified gel retardation assays and UV analysis of the complexes.

The association with cells is vital for NP-aided siRNA delivery.<sup>43-45</sup> The protamine:siRNA complexation to the Au NPs, as mentioned above, does not have a significant effect on the toxicity of the Au NPs. Protamine:siRNA on its own also does not exhibit any toxicity. In addition the protamine:siRNA complex at the MR used here does not display and knockdown effects when not complexed with Au NPs. The MR used was chosen as it introduces the charge change necessary for interaction with the Au NPs rather than for any inherent transfection effects. However, the siRNA-protamine loading used here is sufficient for transfection studies.<sup>45</sup> To examine this, fluorescent siRNA was complexed with PEG-Au nanoparticles as before, and their association with CT26 cells was assessed by fluorescence microscopy (**Figure 6**).<sup>46,47</sup> All of the tested Au NP formulations showed a good level of interaction, as evidenced by the green staining in the images (5b-d). Protamine condensed siRNA alone showed negligible uptake (**Figure 6a**) indicating the inability of siRNA alone to associate with cells. Transfection efficiency and gene silencing can be determined by measuring the reduction in the expression of a reporter gene, such as luciferase. GL3 luciferase siRNA was condensed with protamine and complexed with the PEG-Au nanoparticles. Knockdown in levels of luciferase protein expression<sup>48</sup> was seen with all of the PEG-Au complexes (30-50 %) (**Figure 7**) and significant knockdown, compared with the untreated control was seen with 4 particles; 15 nm-PEG<sub>2,000</sub>, 15 nm-PEG<sub>5,400</sub>, 30 nm-PEG<sub>10,800</sub> and 60 nm-PEG<sub>10,800</sub> ( $p < 0.05$  – Student T Test). This compares favourably with the commercial siRNA delivery vector, Lipofectamine 2000, which achieved knockdown of ~60 %. No significant knockdown was observed with non silencing siRNA, confirming the specific nature of the siRNA. None of the PEG-Au NPs synthesised in this study exhibited any cytotoxicity in CT-26 cell cultures, either alone or when complexed with siRNA. The slightly negatively charged PEG-Au NPs produced in this study were able to interact electrostatically with protamine condensed fluorescent siRNA, allowing cellular association of the complexes to be monitored by fluorescence microscopy.

The physical characteristics of the PEG-Au NPs were conserved after complexation with siRNA/protamine, as no change in the colour of the colloidal solutions was observed after bioconjugation. However, a slight increase in the size of the NPs after complexation with siRNA/protamine was detected by DLS, most likely due to weak interactions between neighboured nanoparticles; however, this interaction was not strong enough to release the ligands from the surface of the nanoparticles to allow direct core-core interaction. A net positive charge was measured for the Au NPs complexed with siRNA/protamine, making these suitable candidates for cellular delivery by interaction with the negatively charged plasma membrane. Data from cell association, as determined by fluorescence, and siRNA delivery, as determined by luciferase knockdown indicate that the particles are effective at associating with and entering cells.

## Conclusions

Electrostatically-stabilised Au NPs-citrate have very limited applications due to its fast aggregation in complex media such as the presence of high concentration of salts that is the main cause of this aggregation. However, steric stabilisation of Au NPs with PEG polymer offers a high degree of stability to the Au NPs dispersion. Au NPs-PEG hybrids were shown here to catalyse aryl homocoupling reactions in water, although no clear conversion was observed with 60 nm diameter NPs. The yield of the homocoupling reaction of *p*-methoxyphenyl boronic was found to increase with Au NPs-PEG loading, demonstrating the catalytic efficacy of the Au NPs-PEG in the catalytic homocoupling of boronic acids. Finally, all of the Au NP-PEG hybrids tested here were checked for cytotoxicity on B16.F10 and CT26 cell lines, and were found to be not cytotoxic and able to deliver siRNA into the cells. Further studies to attach biomolecules on PEG-AuNPs and their interactions with platelet are now in progress in order to use these NPs in active targeting and receptor mediated delivery.

**ACKNOWLEDGMENT** We acknowledge financial support from Science Foundation Ireland (Grant 07/SRC/B1155 and 07/SRC/B1154 ) to the Irish Drug Delivery network (IDDN) through Strategic

Research Cluster (SRC) grants. This research was also enabled by the Higher Education Authority Program for Research in Third Level Institutions (2007-2011) via the INSPIRE programme. Microscopy analysis was undertaken at the Electron Microscopy and Analysis Facility (EMAF) at the Tyndall National Institute, Cork, Ireland.

## FIGURES AND SUPPORTING INFORMATION

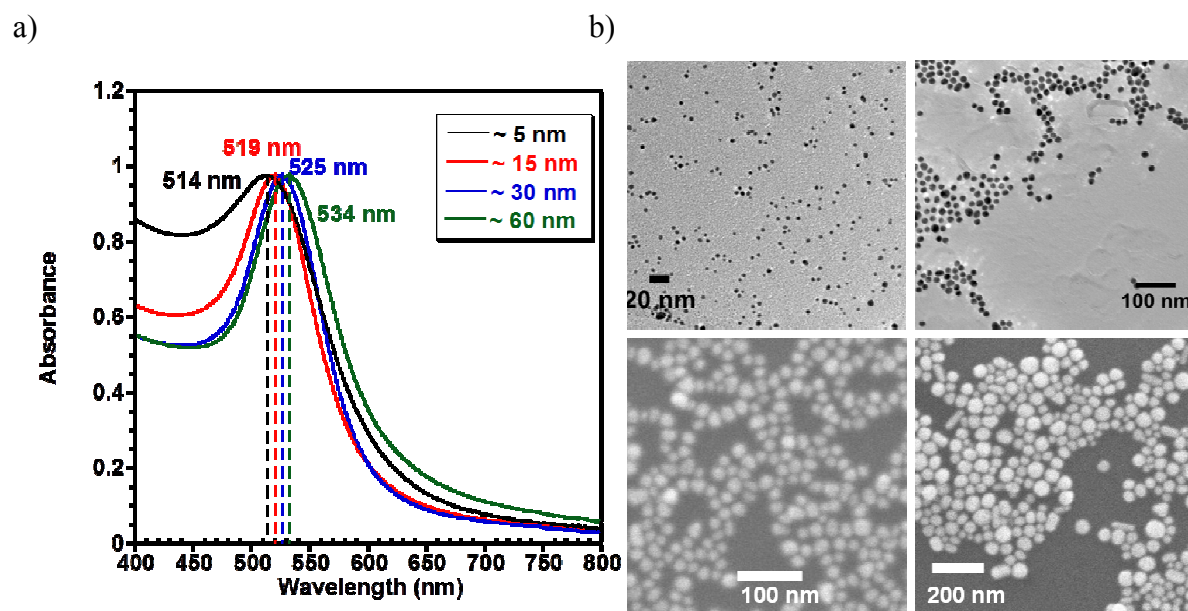


**Figure 1.** a) UV-visible spectra, and b) TEM/SEM micrographs (up right) of the AuNPs-Citrate with diameter ~5 nm (up left); ~15 nm (up right); 30 nm (down left) and 60 nm (down right) obtained in this study.

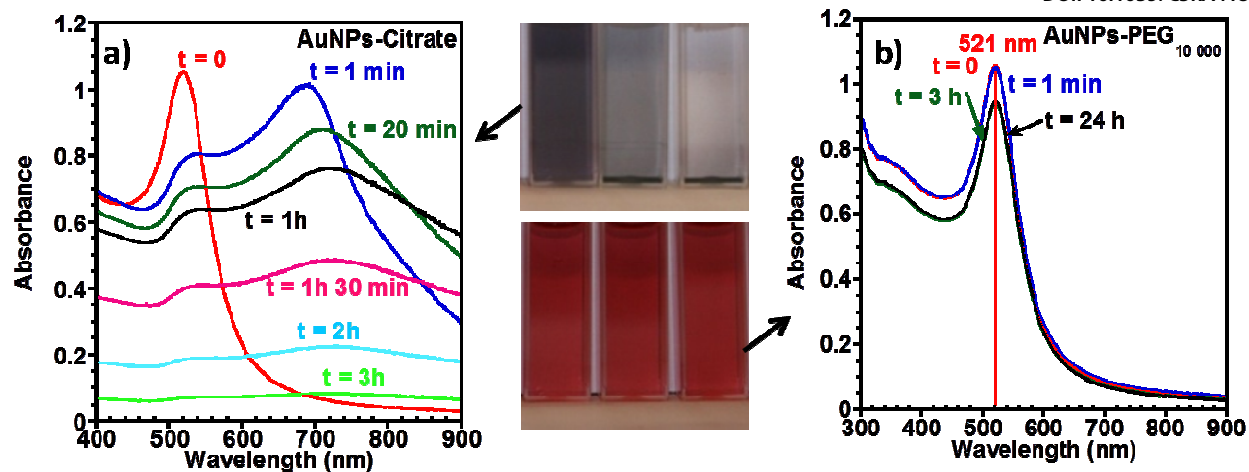


**Figure 2.** Effect of salt (0.157 M NaCl) followed by UV-visible spectroscopy. (a) AuNPs-citrate, (b) AuNPs-PEG<sub>10 000</sub>. The pictures of the colloidal solutions in the middle show the high stability of the PEG-AuNPs colloidal solution in high ionic strength conditions, compared to AuNPs-citrate that are aggregated and precipitated.

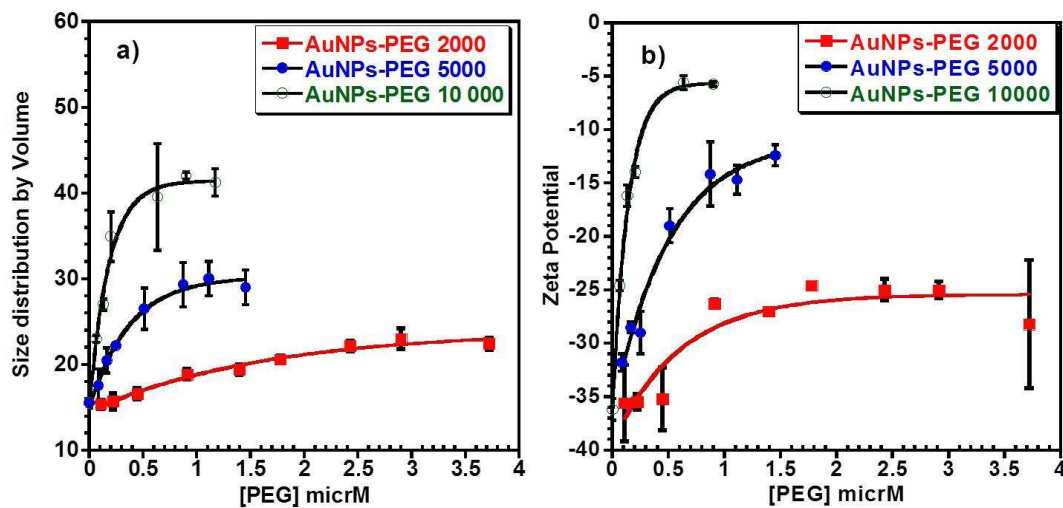


**Figure 3.** (a) Size distribution by volume and zeta potential (b) of 15 nm AuNPs-PEG hybrids as a function of mPEG-SH polymer concentration expressed in  $\mu\text{mol L}^{-1}$ , for mPEG-SH with MW 2100; 5400; and 10 800  $\text{g}\cdot\text{mol}^{-1}$ .

Boronic acid	PEG size	Base	Au size	Time/Temp	Ratio of products by <sup>1</sup> H NMR: SM:Homocoupled product: <i>p</i> MeO-phenol
MeO-PhB(OH) <sub>2</sub>	10000	NaOH	6 nm	80°C/25 h	0:1:4.9
MeO-PhB(OH) <sub>2</sub>	10000	NaOH	30 nm	80°C/25 h	0:1:10.3
MeO-PhB(OH) <sub>2</sub>	10000	NaOH	~ 60 nm	80°C/25 h	1:1:23
MeO-PhB(OH) <sub>2</sub>	5000	NaOH	15 nm	80°C/25 h	0:1:4.7
MeO-PhB(OH) <sub>2</sub>	20000	NaOH	15 nm	80°C/25 h	0:1:4.5
<sup>a</sup> MeO-PhB(OH) <sub>2</sub>	20000	Na <sub>2</sub> CO <sub>3</sub>	15 nm	80°C/25 h	30:1:0
<sup>b</sup> MeO-PhB(OH) <sub>2</sub>	20000	Na <sub>2</sub> CO <sub>3</sub>	15 nm	80°C/25 h	2.1:1:0.4
MeO-PhB(OH) <sub>2</sub>	5000	Cs <sub>2</sub> CO <sub>3</sub>	15 nm	80°C/20 h	4.6:1:7

<sup>a</sup>Solvent EtOH/water <sup>b</sup>Solvent toluene

**Table 1.** Homocoupling of MeO-PhB(OH)<sub>2</sub> whereby MeO-PhB(OH)<sub>2</sub> and PhBr were heated in the presence of NaOH and water.

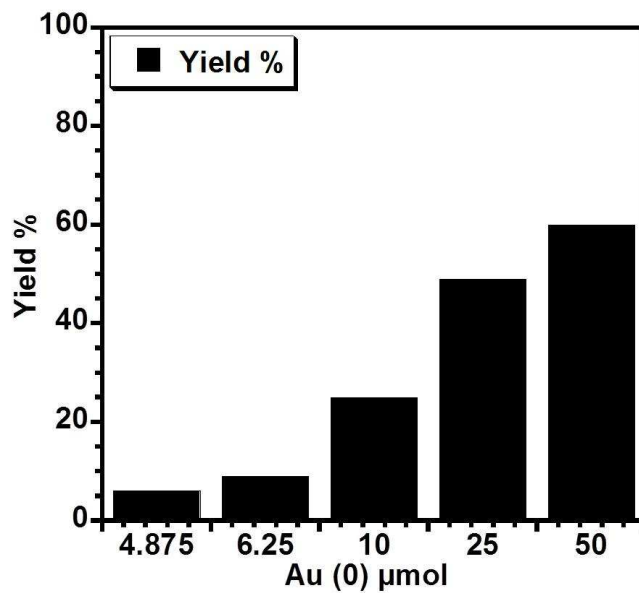


**Figure 4.** Effect of catalyst concentration on the isolated yield for the homocoupling of *p*-methoxyphenyl boronic acid alone.

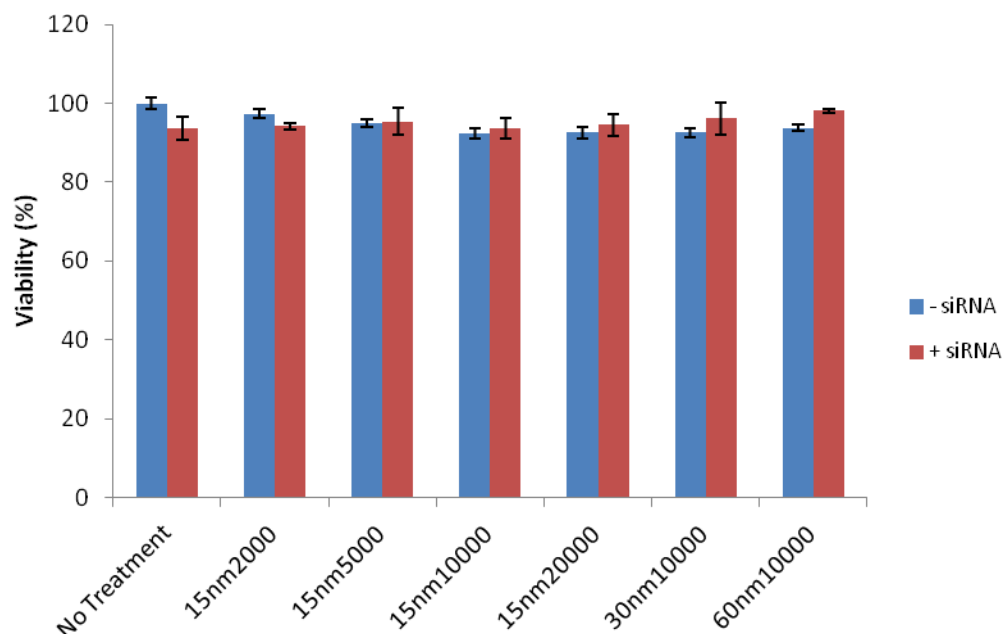


**Figure 5.** Effect of Au-PEG complexes on B16.F10 cell viability. Cells were incubated with a range of Au-PEG:(siRNA:Protamine) complexes or Au-PEG alone at a MR of 1:10 for 4 hours at 37°C. A MTT assay was subsequently carried out and cell viability is expressed as % of dehydrogenase activity relative to untreated control.

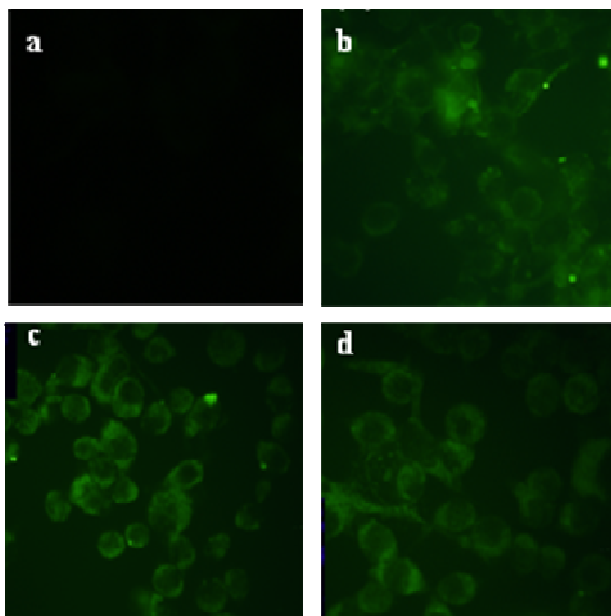


**Figure 6.** Cellular association of Au NP-PEG complexed siRNA with CT26 assessed by fluorescent detection of labeled siRNA using a Nikon Eclipse TS100 inverted microscope equipped with fluorescein and DAPI filters and Metamorph version 6.1 software. Cells were treated (a) with protamine condensed siRNA (MR 1:5) alone (b) 15 nm AuNPs-PEG<sub>2,100</sub>:(protamine:siRNA), (c) 15 nm Au NPs-PEG<sub>5,400</sub>:(protamine:siRNA), (d) 60 nm AuNPs-PEG<sub>10800</sub>:(protamine:siRNA). All Au NPs were complexed at a MR 10. 20 hours post transfection cells were fixed with PFA and stained with DAPI to visualise the nucleus.

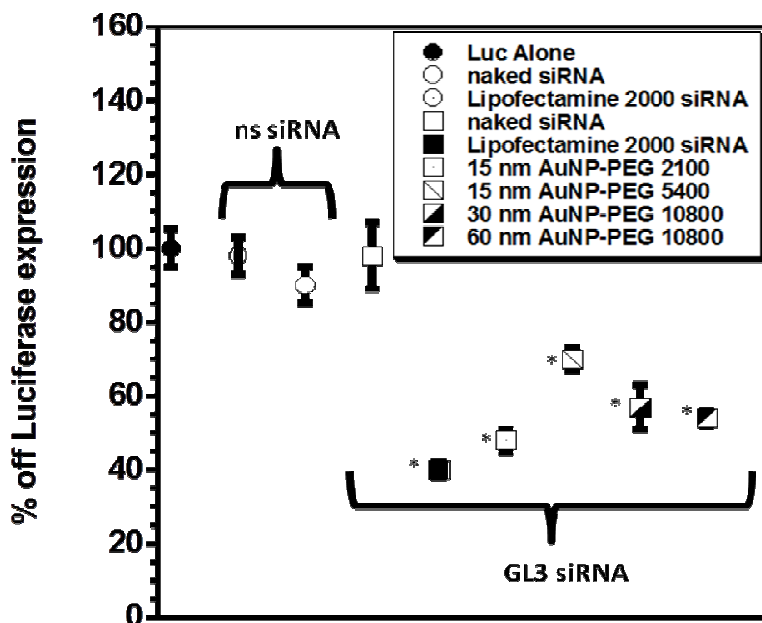
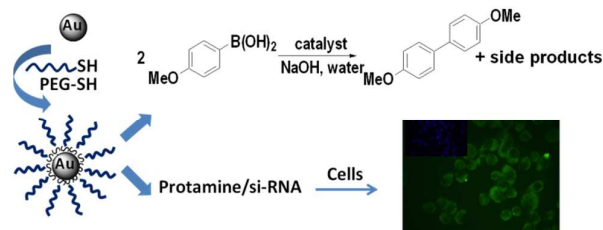


**Figure 7.** siRNA knockdown of Luciferase expression in CT26 cells with Au NPs. CT26 cells were transfected with pGL3 Luciferase plasmid for 2 hours prior to treatment with GL3 siRNA complexed with Au NP's. Luciferase expression was determined 24 hours post siRNA transfection and is expressed as % of non-siRNA treated cells. (Results  $\pm$  SEM of triplicate data) (\* $p < 0.05$ ).

## REFERENCES

1. M. C. Daniel and D. Astruc, *Chem. Rev.*, 2004, **104**, 293-346.
2. A. Corma and H. Garcia, *Chem. Soc. Rev.*, 2008, **37**, 2096-2126.
3. B. I. Lee, L. Qi and T. Copeland, *J. Ceram. Process. Res.*, 2005, **6**, 31-40.
4. S. Link and M. A. El-Sayed, *J. Phys. Chem. B*, 1999, **103**, 4212-4217.
5. K. S. Lee and M. A. El-Sayed, *J. Phys. Chem. B*, 2006, **110**, 19220-19225.
6. Y. E. K. Lee and R. Kopelman, *Imaging and Spectroscopic Analysis of Living Cells: Optical and Spectroscopic Techniques, UK: Academic Press*, 2012, **504**, 419-470.
7. P. Zrazhevskiy and X. Gao, *Miner. Biotech.*, 2009, **21**, 37-52.
8. S. K. Nune, P. Gunda, P. K. Thallapally, Y. Y. Lin, M. L. Forrest and C. J. Berkland, *Expert Opin. Drug Deliv.*, 2009, **6**, 1175-1194.
9. R. M. Mohamed, D. L. McKinney and W. M. Sigmund, *Mater. Sci. & Eng. R-Reports*, 2012, **73**, 1-13.
10. C. J. Murphy, T. K. San, A. M. Gole, C. J. Orendorff, J. X. Gao, L. Gou, S. E. Hunyadi and T. Li, *J. Phys. Chem. B*, 2005, **109**, 13857-13870.
11. C. J. Orendorff, T. K. Sau and C. J. Murphy, *Small*, 2006, **2**, 636-639.
12. K. Rahme, F. Gauffre, J. D. Marty, B. Payre and C. Mingotaud, *J. Phys. Chem. C*, 2007, **111**, 7273-7279.
13. R. A. Sperling, P. Rivera gil, F. Zhang, M. Zanella and W. J. Parak, *Chem. Soc. Rev.*, 2008, **37**, 1896-1908.
14. A. Abad, P. Conceptiòn, A. Corma and H. Garcia, *Angew. Chem. Int. Ed.*, 2005, **44**, 4066-4069.
15. D. I. Enache, J. K. Edwards, P. Landon, B. Solsona-Espriu, A. F. Carley, A. A. Herzing, M. Watanabe, C. J. Kiely, D. W. Knight and G. J. Hutchings, *Science*, 2006, **311**, 362-365.
16. H. Miyamura, R. Matsubara, Y. Miyazaki and S. Kobayashi, *Angew. Chem. Int. Ed.*, 2007, **46**, 4151-4154.
17. M. Haruta, N. Yamada, T. Kobayashi and S. Iijima, *J. Catal.*, 1989, **115**, 301-309.
18. J. Guzman and B. C. Gates, *J. Am. Chem. Soc.*, 2004, **126**, 2672-2673.
19. C. Lemire, R. Meyer, S. Shaikhutdino and H. J. Freund, *Angew. Chem. Int. Ed.*, 2004, **43**, 118-121.
20. A. Corma, *Science*, 2006, **313**, 332-334.
21. G. C. Bond, C. Louis and D. T. Thompson, *Catalysis by Gold*, Imperial College Press, 2006.
22. A. Arcadi and S. Di Giuseppe, *Curr. Org. Chem.*, 2004, **8**, 795-812.
23. A. S. K. Hashmi and G. H. Hutchings, *Angew. Chem. Int. Ed.*, 2006, **45**, 7896-7936.
24. J. Hamn, Y. Liu and R. Guo, *J. Am. Chem. Soc.*, 2009, **131**, 2060-2061.
25. B. Karimi and F. K. Esfahani, *Chem. Commun.*, 2011, **47**, 10452-10454.
26. S. Carrettin, J. Guzman and A. Corma, *Angew. Chem. Int. Ed.*, 2005, **44**, 2242-2245.
27. Y. J. Liang, M. Ozawa and A. Krueger, *Acs Nano*, 2009, **3**, 2288-2296.
28. I. Romer, T. A. White, M. Baalousha, K. Chipman, M. R. Viant and J. R. Lead, *J. Chromatogr. A*, 2011, **1218**, 4226-4233.
29. K. Rahme, P. Vicendo, C. Ayela, C. Gaillard, B. Payre, C. Mingotaud and F. Gauffre, *Chem.-Eur. J.*, 2009, **15**, 11151-11159.
30. H. Otsuka, Y. Nagasaki and K. Kataoka, *Adv. Drug Deliv. Rev.*, 2003, **55**, 403-419.
31. J. Rubio-Garcia, Y. Coppel, P. Lecante, C. Mingotaud, B. Chaudret, F. Gauffre and M. L. Kahn, *Chem. Commun.*, 2011, **47**, 988-990.
32. F. Ullmann and J. Bielecki, *Chem. Ber.*, 1901, **34**, 2174-2185.
33. D. A. Horton, G. T. Bourne and M. L. Smythe, *Chem. Rev.*, 2003, **103**, 893-930.
34. D. A. Fleming and M. E. Williams, *Langmuir*, 2004, **20**, 3021-3023.
35. G. Frens, *Nature-Phys. Sci.*, 1973, **241**, 20-22.
36. J. Kimling, M. Maier, B. Okenve, V. Kotaidis, H. Ballot and A. Plech, *J. Phys. Chem. B*, 2006, **110**, 15700-15707.

37. J. Turkevich, P. C. Stevenson and J. Hillier, *Discuss. Faraday. Soc.*, 1951, **11**, 55-75.
38. S. Sistach, K. Rahme, N. Perignon, J. D. Marty, N. L. D. Viguerie, F. Gauffre and C. Mingotaud, *Chem. Mater.*, 2008, **20**, 1221-1223.
39. K. Rahme, L. Chen, R. G. Hobbs, M. A. Morris, C. O'Driscoll and a. J. D. Holmes, *RSC Advances*, 2013, **3**, 6085-6094.
40. K. Rahme, J. Oberdisse, R. Schweins, C. Gaillard, J. D. Marty, C. Mingotaud and F. Gauffre, *Chemphyschem.*, 2008, **9**, 2230-2236.
41. M. S. Suh, G. Shim, H. Y. Lee, S.-E. Han, Y.-H. Yu, Y. Choi, K. Kim, I. C. Kwon, K. Y. Weon, Y. B. Kim, Y.-K. Oh, *J. Control. Release*, 2009, **140**, 268-276.
42. Y. H. Yu, E. Kim, D. E. Park, G. Shim, S. Lee, Y. B. Kim, C.-W. Kim, Y.-K. Oh, *Eur. J. Pharm. Biopharm.*, 2012, **80**, 268-273.
43. X.-Z. Yang, S. Dou, T.-M. Sun, C.-Q. Mao, H.-X. Wang, J. Wang, *J Control. Release*, 2011, **156**, 203-211.
44. J. Zhou, K.-T. Shum, J. C. Burnett and J. J. Rossi, *Pharmaceuticals* 2013, **6**, 85-107.
45. P. Guo, O. Coban, N. M. Snead, J. Trebley, S. Hoeprich, S. Guo, and Y. Shu, *Adv. Drug Deliv. Rev.*, 2010, **62**, 650-666.
46. V. Sée, P. Free, Y. Cesbron, P. Nativo, U. Shaheen, D. J. Rigden, D. G. Spiller, D. G. Fernig, M. R. H. White, I. A. Prior, M. Brust, B. Lounis and R. Lévy, *ACS Nano*, 2009, **3**, 2461-2468.
47. R. Lévy, U. Shaheen, Y. Cesbron and V. Sée, *Nano Rev.*, 2010, **1**, 4889 – 4907.
48. Y. Kamachi, Y. Okuda, H. Kondoh, *Genesis*, 2008, **46**, 1-7.



PEG modified Gold Nanoparticles as useful tool to catalyze homocoupling reaction of 4-methoxyphenylboronic acid, and to deliver si-RNA to Cells.